Available online at www.sciencedirect.com

SCIENCE DIRECT®

Chemical Physics Letters 396 (2004) 38–42

CHEMICAL PHYSICS LETTERS

www.elsevier.com/locate/cplett

# Surface energetics of hydroxyapatite: a DFT study

Weihua Zhu, Ping Wu *

*Institute of High Performance Computing, 1 Science Park Road, # 01-01 The Capricorn, Singapore Science Park II, Singapore 117528, Singapore*

Received 27 May 2004; in final form 6 August 2004
Available online 24 August 2004

**Abstract**

The surface energetics of hydroxyapatite was studied using density functional theory within the generalized gradient approximation. The effects of slab thickness, vacuum width between slabs and surface relaxation on surface energy have been tested. The results show that as long as the vacuum width is 12 Å or more, the influence of vacuum width on surface energy is small. Slabs with a thickness of 15.6 Å are enough to obtain meaningful results. Relaxation of the slab surfaces has an apparent effect on surface energy. Surface relaxation modifies the relative order of the morphological importance compared with unrelaxation.

## 1. Introduction

Hydroxyapatite $Ca_{10}(PO_4)_6(OH)_2$ is the basic mineral component of mammalian bones and tooth enamel [1]. Recently it has attracted considerable interests due to its applications in the repair, reconstruction, and replacement of diseases or damaged parts of the body as an important bioactive ceramic material [2–4]. Besides its application in medicine and dentistry as a substitute for calcified tissue, it is proposed as an environmental adsorbent of metals and as a catalyst [5,6]. As apatites are important materials with applications in medical prostheses, environmental remediation and catalysis, it is of basic interest to understand the crystal formation [7], dissolution processes [8] and interfacial interactions between the crystalline and amorphous phases. The surface property of the apatite is of direct relevance for these processes. Thus there is a clear need to gain an understanding of the surface energetics of hydroxyapatite.

Theoretical calculations that employ periodic boundary conditions are an effective way to model the physical and chemical properties of complex solids at atomic level as a complement to experimental work. It is recognized that atomistic simulations based on well-defined classical force fields provide a feasible basis for analyzing and predicting structure and properties of hydroxyapatite and other complex analogues [9–14]. Recently density functional theory (DFT) using pseudopotentials and a plane wave basis set, often used within the generalized gradient approximation (GGA), is well established and has been successfully applied to the study of structure and properties of hydroxyapatite and other apatites [15–18]. Although hydroxyapatite and other apatites are the subject of extensive theoretical studies, investigation on the surface energetics of hydroxyapatite is still scarce.

In this Letter, we perform periodic DFT total energy calculations to study the energetics of the hydroxyapatite surfaces by using slab model. Particular emphasis is placed on the technical aspects of the calculations. These include the slab thickness, the vacuum width between slabs and the surface relaxation. Then we investigate the energetics of several low-index hydroxyapatite surfaces.

---

* Corresponding author. Fax: +65 677 80522.
*E-mail address:* wuping@ihpc.a-star.edu.sg (P. Wu).

0009-2614/$ - see front matter © 2004 Elsevier B.V. All rights reserved.
doi:10.1016/j.cplett.2004.08.006

## 2. Computational details

The calculations performed in this study within the framework of DFT were done using Vienna ab initio simulation program (VASP) and the ultrasoft pseudopotential database contained therein [19–21]. The interaction between ions and electrons is described by fully nonlocal optimized ultrasoft pseudopotentials similar to those introduced by Vanderbilt [22,23]. These pseudopotentials allow a smaller basis set for a given accuracy. The residual minimization technique [21] is used to calculate the electronic ground state. The relaxation of different atomic configures was based on a conjugate-gradient (CG) minimization [19] of the total energy. The surface structures are considered to be in equilibrium when the Hellmann–Feynman forces exerted on the atoms are smaller than 0.002 eV/Å. The GGA proposed by Perdew and Wang [24], named PW91, was employed. The cutoff energy of plane waves was set to 500 eV. Brillouin zone sampling for slab surface was performed using the Monkhost–Pack scheme with a *k*-point grid of $2 \times 2 \times 1$ ($2 \times 2 \times 2$ for bulk). The values of $E_{\mathrm{cut}}$ and the *k*-point grid were determined to ensure the convergence of total energies to within 0.01%. These results are supported by other studies [16,17].

To model the hydroxyapatite surface at periodic boundary conditions, a slab of finite thickness perpendicular to the surface but infinite extension in the other two directions was used. Slabs are separated from repeated replicas by a certain vacuum width. These slab surfaces were obtained by cleaving hydroxyapatite crystal.

We used surface energy method to predict the surface energetics of hydroxyapatite. The surface energy is calculated from the difference in energy of the surface ions to those in the bulk per unit surface area

$$E_{\mathrm{surf}} = (E_{\mathrm{slab}} - nE_{\mathrm{bulk}})/A, \tag{1}$$

where $E_{\mathrm{surf}}$ is the surface energy, $E_{\mathrm{slab}}$ the total energy per repeated slab supercell, $E_{\mathrm{bulk}}$ the energy per unit cell in the bulk, $n$ the number of unit cells and $A$ the total surface area per repeated unit. For a crystal in equilibrium with its surroundings, the surface energy must be minimal for a given volume. Hence the morphological importance of a face is inversely proportional to the surface energy [25].

According to above knowledge, the relative growth rate $R$ is defined as

$$R = X(hkl)/X(h'k'l'), \tag{2}$$

where $X(h\,k\,l)$ and $X(h'\,k'\,l')$ stand for surface energy $E_{\mathrm{surf}}$ for the faces of Miller indexes ($h\,k\,l$) and ($h'\,h'\,k'\,h'\,l'$), respectively. Thus, faces with the lowest relative growth rate have the most morphological importance.

Eq. (1) gives good results only if the bulk energy ($E_{\mathrm{bulk}}$) is accurately calculated. The most straightforward way to extract the quantity $E_{\mathrm{bulk}}$ is to fit a straight line of the slab total energy values versus the slab thickness $n$ (except for in the case of the thinnest slab) and to take the slope [26]

$$E_{\mathrm{slab}} = AE_{\mathrm{surf}} + nE_{\mathrm{bulk}}. \tag{3}$$

In the system studied here, the dependence is essentially linear already for very thin slabs. Except for the thinnest slab, when starting the fit at different *n*s in the range from 2 to 6, the difference in $E_{\mathrm{bulk}}$ is 0.01 eV. The surface energies given below correspond to energy fits for the range $n$ = 3–6.

## 3. Results and discussion

### 3.1. Bulk properties of hydroxyapatite

In order to benchmark the accuracy of the method for our surface calculations, we carried out initial tests on the bulk hydroxyapatite system. Biological and natural hydroxyapatite has a hexagonal crystal structure with space group $P6_3/m$ [27], with one formula unit $Ca_{10}(PO_4)_6(OH)_2$ per unit cell. As represented in Fig. 1a, calcium ions are situated in two different sites, Ca(1) at site 1 which is coordinated to nine oxygen ions situated in six different phosphate tetrahedral and Ca(2) at site 2 which is 7-fold coordinated by six oxygen ions of five phosphate groups and the hydroxyl ion. The Ca(2) ions are distributed in a hexagonal screw configuration along the *c*-axes forming tunnels whose center is occupied by an array of hydroxyl ions. Considering the different sites at which the Ca and O ions are found, the above formula may be rewritten as $Ca(1)_4Ca(2)_6[PO(1)O(2)O(3)_2]_6(O_HH)_2$. The arrangement of these ions on planes perpendicular to the *c*-axis is presented in Fig. 1b.

The full relaxation of the structure was performed to allow the cell shape and ionic configurations to change at a fixed cell volume. The calculated structural parameters and bond lengths of bulk hydroxyapatite are given in Table 1. It is found that the bulk structures of hydroxyapatite are well reproduced. We obtain the lattice constants $a = b = 9.520$, $c = 6.874$ Å, in good agreement with the experiment values $a = b = 9.432$, $c = 6.881$ Å [27]. Our calculated results are also close to the calculated values $a = b = 9.563$, $c = 6.832$ Å obtained by de Leeuw [16] using DFT. In order to check the effect of the relaxation on the ion configurations, we compared relaxed atomic fractional coordinates for hydroxyapatite unit cell with experimental results in Table 1. The results show that the effect of the relaxation on the ionic positions is very small. The internal structure parameters of hydroxyapatite assigned by the bond lengths are very close to the experimental data. These comparisons confirm that our computational parameters are reasonably satisfactory.

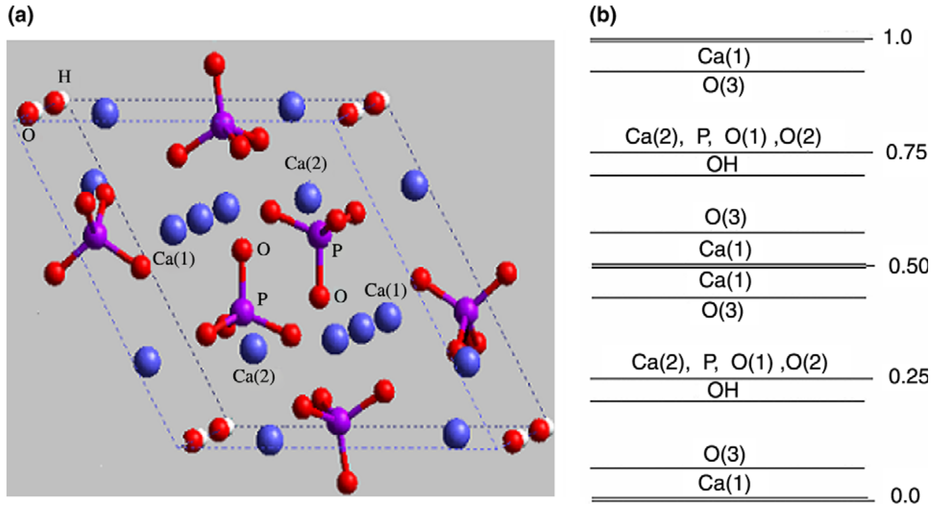

Fig. 1. (a) Hydroxyapatite $Ca_{10}(PO_4)_6(OH)_2$ unit cell; (b) schematic representation of ions stacking order along the $c$ axis.

Table 1
Comparison of relaxed lattice constants (Å), atomic fractional coordinates and bond lengths (Å) for hydroxyapatite with experimental results

| | Lattice parameters | | | | | |
|---|---|---|---|---|---|---|
| | DFT | | | Experiment[a] | | |
| | $a$ | $b$ | $c$ | $a$ | $b$ | $c$ |
| | 9.520 | 9.520 | 6.874 | 9.432 | 9.432 | 6.881 |
| | Atomic fractional coordinates | | | | | |
| | $x$ | $y$ | $z$ | $x$ | $y$ | $z$ |
| Ca(1) | 0.333 | 0.667 | 0.003 | 0.333 | 0.667 | 0.001 |
| Ca(2) | 0.251 | 1.000 | 0.250 | 0.246 | 0.993 | 0.250 |
| P | 0.400 | 0.369 | 0.252 | 0.400 | 0.369 | 0.250 |
| O(1) | 0.333 | 0.487 | 0.253 | 0.329 | 0.484 | 0.250 |
| O(2) | 0.588 | 0.463 | 0.247 | 0.589 | 0.466 | 0.250 |
| O(3) | 0.338 | 0.256 | 0.073 | 0.348 | 0.259 | 0.073 |
| $O_H$ | 0.000 | 0.000 | 0.285 | 0.000 | 0.000 | 0.250 |
| *Bond lengths* | | | | | | |
| P–O(1) | 1.541 | | | 1.533 | | |
| P–O(2) | 1.554 | | | 1.544 | | |
| P–O(3) | 1.545 | | | 1.514 | | |
| Ca(1)–O(1) | 2.425 | | | 2.416 | | |
| Ca(1)–O(2) | 2.469 | | | 2.449 | | |
| Ca(1)–O(3) | 2.827 | | | 2.802 | | |
| Ca(1)–$O_H$ | 2.357 | | | 2.354 | | |
| Ca(2)–O(1) | 2.798 | | | 2.712 | | |
| Ca(2)–O(2) | 2.357 | | | 2.356 | | |
| Ca(2)–O(3) | 2.367 | | | 2.367 | | |
| Ca(2)–$O_H$ | 2.510 | | | 2.511 | | |

[a] Ref. [26].

### 3.2. Convergence tests for slab surface

To ensure that the results of the calculation accurately represent an isolated surface, the vacuum regions must be wide enough so that faces of adjacent crystal slabs do not interact across the vacuum region, and the crystal slab must be thick enough so that the two surfaces of each crystal slab do not interact through the bulk crystal. Therefore it is important to test the convergence of vacuum width and slab thickness. As a compromise between computation efficiency and accuracy, only (1 0 0) surface is considered as an example for these tests. The model of one-layer slab is shown in Fig. 2. The thickness of the slabs is usually expressed in terms of a number of layers, where one layer is defined as the depth of one unit cell that contains 44 atoms.

Fig. 3 presents the variation of surface energy as a function of vacuum width for slab thicknesses of 1 and 2 layers. With increasing vacuum width, the evolution pattern of surface energy for slab thicknesses of 1 and 2 layers is very similar. The vacuum width has a marked effect on the surface energy for vacuum widths smaller than 6.0 Å, but a small effect for vacuum widths larger than 6.0 Å. The differences in the surface energy of slab

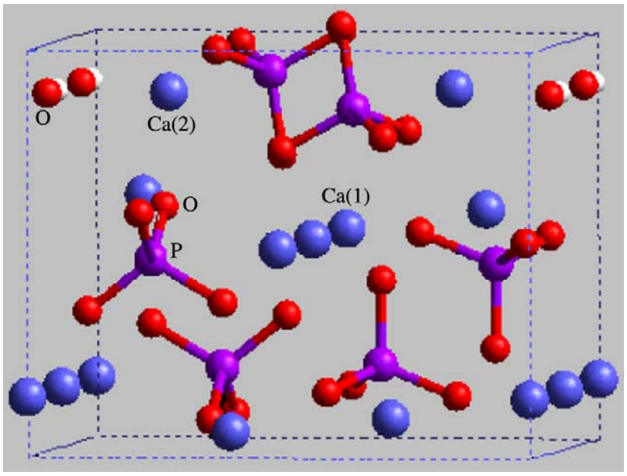

Fig. 2. One-layer slab model for hydroxyapatite (1 0 0) surface. The slab is repeated in the $z$ direction and separated by vacuum layer.

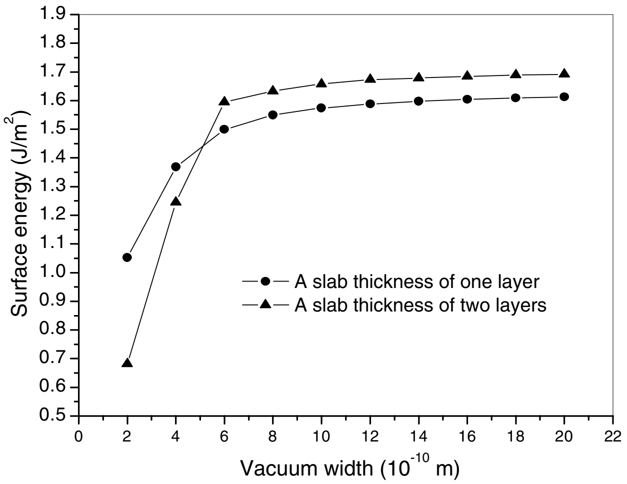

Fig. 3. The variation of (1 0 0) surface energy as a function of vacuum width for slab thicknesses of 1 and 2 layers.

thicknesses of 1 and 2 layers are small for vacuum widths larger than 6.0 Å. Slab thicknesses of 1 and 2 layers have a similar effect on their surface energy of these slabs with different vacuum width. We note from Fig. 3 that the vacuum width of 12.0 Å is enough to obtain meaningful results. Vacuum widths of 20.0 Å are used in all subsequent calculations.

To investigate the effect of structure relaxation on surface energy, all the ions in slab supercells are allowed to relax at a fixed cell shape and volume. Fig. 4 displays the evolution of (1 0 0) surface energy with the increment of slab thickness under unrelaxation and relaxation. The calculated results show that the slab thickness has a bit effect on the surface energy at first, but convergence to the infinite limit is rapid. Considered the relaxation effects, the variation trend of the surface energy with increment of slab thickness is similar to the unrelaxed results. It can be seen from Fig. 4 that surface relaxation has a marked effect on the surface energies. Compared with unrelaxed values, surface relaxation lowers the surface energies by about 80%. We explicitly consider the effects of atomic relaxation on the surface energy in the subsequent calculations. From above discussion, we regard two-layer slabs (about 15.6 Å) as the minimum thickness needed to obtain meaningful results. Slabs with a thickness of 15.6 Å are used to calculate the surface energy in our further calculations.

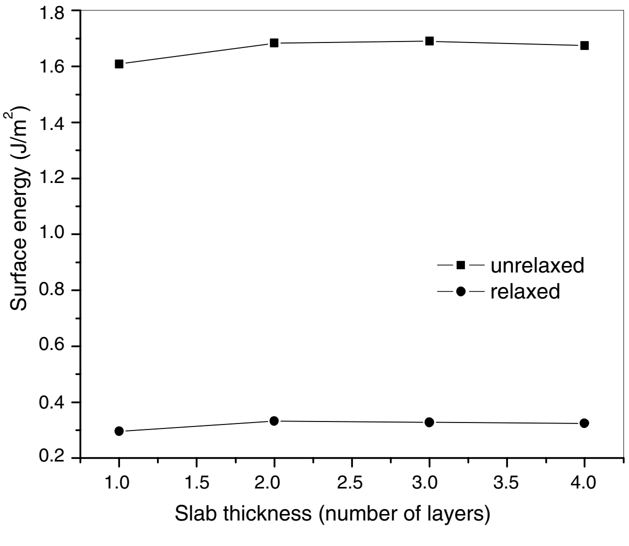

Fig. 4. The evolution of (1 0 0) surface energy with increasing slab thickness.

### 3.3. Surface energetics

The external morphology of crystalline materials from the internal crystal structure can be predicted by using surface energy. The faces which are likely to appear in the morphology need to be firstly determined so that the following calculations can be performed on them. The Bravais–Friedel–Donnay–Harker (BFDH) morphological prediction method of Cerius2 [28] was used to create several low Miller index surfaces of hydroxyapatite studied here. The BFDH method is a geometrical calculation that uses the crystal lattice and symmetry to generate a list of possible growth faces and their relative growth rates [29,30]. From this, crystal morphology can be deduced. The method is an approximation, and does not account for the energetics of the system. Table 2 gives the calculated surface energies and relative growth rates for different Miller index ($h\,k\,l$) slab faces of hydroxyapatite at DFT level.

The order of morphological importance predicted by the BFDH method is: $(1\,0\,0) > (\bar{1}\,0\,0) > (\bar{1}\,1\,0) > (0\,1\,0) > (0\,\bar{1}\,0) > (1\,\bar{1}\,0)$. It is found that the $(1\,0\,0)$, $(\bar{1}\,0\,0)$ and $(\bar{1}\,1\,0)$ surfaces have the most morphological importance. Without considering surface relaxation, the surface energy method at DFT level has predicted the following ordering of the morphological importance: $(1\,0\,0) > (\bar{1}\,0\,0) > (\bar{1}\,1\,0) \sim (1\,\bar{1}\,0) > (0\,1\,0) > (0\,\bar{1}\,0)$. The prediction that most stable three surfaces are $(1\,0\,0), (\bar{1}\,0\,0)$ and $(\bar{1}\,1\,0)$ agrees with that by the BFDH method, but the relative sequence found

Table 2
Calculated surface energies $E_{\mathrm{surf}}$ (J/m$^2$) and relative growth rates ($R$) for different Miller index ($h\,k\,l$) slab faces of hydroxyapatite

| ($h\,k\,l$) | Unrelaxation | | Relaxation | |
|---|---|---|---|---|
| | $E_{\mathrm{surf}}$ | $R$ | $E_{\mathrm{surf}}$ | $R$ |
| $(1\,0\,0)$ | 1.6922 | 1.0000 | 0.3322 | 1.0181 |
| $(\bar{1}\,0\,0)$ | 1.6925 | 1.0001 | 0.3287 | 1.0074 |
| $(\bar{1}\,1\,0)$ | 1.6926 | 1.0002 | 0.3263 | 1.0000 |
| $(0\,1\,0)$ | 1.6928 | 1.0003 | 0.3317 | 1.0165 |
| $(0\,\bar{1}\,0)$ | 1.6929 | 1.0004 | 0.3381 | 1.0362 |
| $(1\,\bar{1}\,0)$ | 1.6926 | 1.0002 | 0.3366 | 1.0316 |

for $(1\,0\,0)$, $(\bar{1}\,0\,0)$ and $(\bar{1}\,1\,0)$ disagrees with the BFDH predictions.

In above section, we note that surface relaxation has an apparent effect on the surface energy. Here the slabs were allowed to fully relax in all directions under the restriction of fixed cell parameters. The results are also listed in Table 2. Considered surface relaxation, the surface energy method based on DFT level has determined the order of the surface stability: $(\bar{1}\,1\,0) > (\bar{1}\,0\,0) > (0\,1\,0) > (1\,0\,0) > (1\,\bar{1}\,0) > (0\,\bar{1}\,0)$. The results show that surface relaxation alters the relative order of the morphological importance compared with unrelaxation. The difference between the unrelaxed and relaxed surface energies can serve as a measure of the size of the relaxation. The degree of surface relaxation decreases in the order: $(0\,\bar{1}\,0) > (1\,\bar{1}\,0) > (1\,0\,0) > (0\,1\,0) > (\bar{1}\,0\,0) > (\bar{1}\,1\,0)$.

The BFDH method is an approximation, and takes no account of the details structure or energetics of a crystal. The stronger the bonding effects in the crystal, the less accurate the method becomes. In many cases, however, one can get good approximations, and the method is always useful for identifying important faces in the growth process. The surface energy method can be used to predict the equilibrium morphology. The equilibrium morphology has been found to agree well with small experimentally grown crystals less than a micron in diameter [31].

Relaxation of the slab surfaces has an apparent effect on surface energy. By contrast, relaxation has been found to reduce the surface energies by as much as 80%. Structure relaxation modifies the relative order of the morphological importance compared with unrelaxation. Our calculations indicate that surface relaxation is important on all the surfaces studied.

## 4. Conclusions

In this study, we have performed periodic DFT total energy calculations to investigate the energetics of the hydroxyapatite surfaces by using slab model. The effects of slab thickness, vacuum width between slabs and surface relaxation on surface energy have been tested. The results show that as long as the vacuum width is 12 Å or more, the influence of vacuum width on surface energy is small. Slabs with a thickness of 15.6 Å are enough to obtain meaningful results. Relaxation of the slab surfaces has a marked effect on surface energy. The order of the morphological importance predicted at DFT level is $(1\,0\,0) > (\bar{1}\,0\,0) > (\bar{1}\,1\,0) \sim (1\,\bar{1}\,0) > (0\,1\,0) > (0\,\bar{1}\,0)$. Considered surface relaxation, the order of the surface stability is as follows: $(\bar{1}\,1\,0) > (\bar{1}\,0\,0) > (0\,1\,0) > (1\,0\,0) > (1\,\bar{1}\,0) > (0\,\bar{1}\,0)$.

## References

[1] T.S.B. Narasaraju, D.E. Phebe, J. Mater. Sci. 31 (1996) 1.

[2] W. Rieger, in: G. Kostorz (Ed.), High-Tech Ceramics, Academic Press, San Diego, CA, 1989, p. 35.

[3] B.D. Ratner, A.S. Hoffman, F.J. Schoen, J.E. Lemons, Biomaterials Science, Academic Press, San Diego, CA, 1996.

[4] L.L. Hench, J. Am. Ceram. Soc. 81 (1998) 1705.

[5] Y. Matsumura, J.B. Moffat, J. Chem. Soc. Faraday Trans. 92 (1996) 1981.

[6] N. Toulhoat, V. Potocek, C. Neskovic, M. Fedoroff, J. Jeanjean, V. Vincent, Radiochim. Acta 74 (1996) 257.

[7] T.J. McCoy, M. Wadhwa, K. Keil, Geochim. Cosmochim. Acta 62 (1999) 1249.

[8] S.K. Lower, P.A. Maurice, S.J. Traina, Geochim. Cosmochim. Acta 63 (1998) 1773.

[9] C. Meis, J.D. Gale, L. Boyer, J. Carpean, D. Gosset, J. Phys. Chem. A 104 (2000) 5380.

[10] A. Chartier, C. Meis, J.D. Gale, Phys. Rev. B 64 (2001) 085110.

[11] J. Terra, M. Jiang, D.E. Ellis, Philos. Mag. A 82 (2002) 2357.

[12] D. Mkhonto, N.H. de Leeuw, J. Mater. Chem. 12 (2002) 2633.

[13] N.H. de Leeuw, D. Mkhonto, C.R.A. Catlow, J. Phys. Chem. B 107 (2003) 1.

[14] N.H. de Leeuw, D. Mkhonto, Chem. Mater. 15 (2003) 1567.

[15] V. Louis-Achille, L. De Windt, M. Defranceschi, Comput. Mater. Sci. 10 (1998) 346.

[16] N.H. de Leeuw, J. Chem. Soc. Chem. Commun. 17 (2001) 1646.

[17] N.H. de Leeuw, Chem. Mater. 14 (2002) 435.

[18] L. Calderín, M.J. Stott, Phys. Rev. B 67 (2003) 134106.

[19] G. Kresse, J. Hafner, Phys. Rev. B 47 (1993) 558.

[20] G. Kresse, J. Furthmüller, Comput. Mater. Sci. 6 (1996) 15.

[21] G. Kresse, J. Furthmüller, Phys. Rev. B 54 (1996) 11169.

[22] D. Vanderbilt, Phys. Rev. B 41 (1990) 7892.

[23] G. Kresse, J. Hafner, J. Phys-Condens. Mater. 6 (1994) 8245.

[24] J.P. Perdew, J.A. Chevary, S.H. Vosko, K.A. Jackson, M.R. Pederson, D.J. Singh, C. Fiolhais, Ibid 46 (1992) 6671.

[25] A.L. Rohl, D.H. Gay, J. Cryst. Growth 166 (1996) 84.

[26] V. Fiorentini, M. Methfessel, J. Phys-Condens. Mater. 8 (1996) 6525.

[27] A.S. Posner, A. Perloff, A.F. Diorio, Acta Cryst. 11 (1958) 308.

[28] Cerius2, Molecular Simulations Inc.: San Diego, 1997.

[29] G. Friedel, Bull. Soc. Franc. Minér 30 (1907) 326.

[30] J.D.H. Donny, D. Harker, Am. Mineral 22 (1937) 446.

[31] C.R.A. Catlow, S.C. Parker, M.P. Allen, Computer Modeling of Fluids, Polymers and Solids, Kluwer, Dordrecht, 1990.